Journal of Hazardous Materials 192 (2011) 277–283

Contents lists available at ScienceDirect

Journal of Hazardous Materials

journal homepage: www.elsevier.com/locate/jhazmat

Effective heavy metal removal from aqueous systems by thiol functionalized magnetic mesoporous silica

Guoliang Li[a], Zongshan Zhao[b], Jiyan Liu[a,*], Guibin Jiang[a]

[a] State Key Laboratory of Environmental Chemistry and Ecotoxicology, Research Center for Eco-Environmental Sciences, Chinese Academy of Sciences, P.O. Box 2871, Beijing 100085, China

[b] Key Laboratory of Marine Chemistry Theory and Technology, Ministry of Education, College of Chemistry and Chemical Engineering, Ocean University of China, 238 Songling Road, Qingdao 266100, China

ARTICLE INFO

Article history:
Received 11 February 2011
Received in revised form 28 April 2011
Accepted 6 May 2011
Available online 12 May 2011

Keywords:
Thiol functionalization
Magnetism
Mesoporous silica
Heavy metal
Adsorption

ABSTRACT

A thiol-functionalized magnetic mesoporous silica material (called SH-mSi@Fe_3O_4), synthesized by a modified Stöber method, has been investigated as a convenient and effective adsorbent for heavy metal ions. Structural characterization by powder X-ray diffraction, N_2 adsorption–desorption isotherm, Fourier transform infrared spectroscopy and elemental analyses confirms the mesoporous structure and the organic moiety content of this adsorbent. The high saturation magnetization (38.4 emu/g) make it easier and faster to be separated from water under a moderate magnetic field. Adsorption kinetics was elucidated by pseudo-second-order kinetic equation and exhibited 3-stage intraparticle diffusion mode. Adsorption isotherms of Hg and Pb fitted well with Langmuir model, exhibiting high adsorption capacity of 260 and 91.5 mg of metal/g of adsorbent, respectively. The distribution coefficients of the tested metal ions between SH-mSi@Fe_3O_4 and different natural water sources (groundwater, lake water, tap water and river water) were above the level of 10^5 mL/g. The material was very stable in different water matrices, even in strong acid and alkaline solutions. Metal-loaded SH-mSi@Fe_3O_4 was able to regenerate in acid solution under ultrasonication. This novel SH-mSi@Fe_3O_4 is suitable for repeated use in heavy metal removal from different water matrices.

1. Introduction

Human exposure to heavy metals has risen dramatically in the past decades as a result of an exponential increase in the use of heavy metals in industrial processes and products. Exposure to elevated levels of heavy metals can directly cause various adverse health effects to humans by impairing mental and neurological functions [1]. Therefore, removal of heavy metals from natural and industrial waste water has been drawing more and more attentions. Numerous technologies, including ion exchange [2,3], membrane separation and adsorption [4–6], have been developed. Among them, adsorption is the most promising and frequently used technique owing to its easy application and superior efficiency.

An ideal adsorbent should have features of strong affinity to target sorbate and large surface area with more binding sites. Therefore, numerous researches have focused on porous adsorbents which have shown significant enhancement in heavy metal removal efficiency. Natural and synthetic zeolites and montmorillonites, which are of porous structure, have been used for heavy metal removal from water under different experimental conditions [7–9]. This kind of adsorbents exhibit good selectivity for a number of cations and show strong ion exchange capacity, the release of their components to water was therefore unavoidable even in moderate condition. Addition of those adsorbents can cause severe change of the physical and chemical properties of waters [8]. As a result, adsorbents with high hydrothermal stability and strong resistibility to harsh environment are needed.

Mesoporous materials, having large surface area and uniform pore distribution, have been extensively studied for its widespread applications in fields of adsorption, catalysis, sensors, semiconductor and separation. Modification with ligand, such as amines [10], carbonates and organosulfides [11–13], on the surface of mesoporous materials is necessary to obtain specific adsorption and larger capacity [14–16]. Thiol group is an excellent ligand because of the strong affinity to various heavy metal ions (Hg^{2+}, Ag^{+} and Pb^{2+}, etc.) as result of Lewis acid–base interactions [17]. Co-condensing of siloxane and organosiloxane is a facile approach to synthesizing thiol functionalized silica which allows higher loading of organic functional groups and more homogeneous surface coverage [18]. Using this method, large amount of thiol groups (4.7 mmol of SH/g material) could be introduced into mesoporous substrates [19]. However, it was found that high loading of thiol

* Corresponding author. Tel.: +86 10 62849334; fax: +86 10 62849339.
E-mail address: liujy@rcees.ac.cn (J. Liu).

0304-3894/$ – see front matter © 2011 Elsevier B.V. All rights reserved.
doi:10.1016/j.jhazmat.2011.05.015

groups does not result in high heavy metal adsorption capacity [19,20]. Porous structure also plays an important role in adsorption of heavy metals for thiol functionalized porous materials. Thiol functionalized porous adsorbents with uniform pore channels and narrow pore distribution were found to demonstrate a high selectivity for Hg(II) while exhibits a negligible affinity to other metal ions [20,21]. Mercier and co-workers postulated that the restricted pore volume might result in unfavorable entropy effect and thus lose its spontaneity adsorption except for Hg(II) [21].

Convenient separation from treated water is the other necessity of a promising adsorbent. The traditional adsorbents, such as activated carbon, ion exchange activated alumina, natural porous minerals and the recently developed functionalized mesoporous adsorbents, are difficult to be separated after water treatment. Conventional methods such as centrifugation, precipitation, filtration and chromatography are not only usually labor-consumptive and uneconomical, but also accessible to malformation such as deformation and inactivation. Therefore, convenient and effective separation methods are in urgent demand. Magnetic materials can be easily and rapidly separated from aqueous solutions under an external magnetic field due to their magnetic property and have the advantages of simplicity, high efficiency and sensitivity as well as low costs. Therefore, introducing Fe_3O_4 which features superparamagnetism into the prepared adsorbent is a good way to resolve the problem of separation. There have been a few reports on preparation of different types of mesoporous adsorbents with magnetic nanocomposites incorporated into the pores [22]. However, magnetic nanoparticles dispersed in the pores of the mesoporous materials could block the pore, and lead to high mass transfer resistance.

In this study, a novel adsorbent with magnetic Fe_3O_4 spherical core and thiol functionalized mesoporous silica shell was developed and used for heavy metal ions removal. This material is different from the ordered mesoporous material, showing a worm-hole like pore structure with large surface area and pore distribution, which avails to avoid the unfavorable entropy effect existing in the ordered mesoporous adsorbent leading to lose its spontaneity adsorption except for certain heavy metal ion. A core–shell structure, with magnetic Fe_3O_4 spheres as the core, and mesoporous silica as the shell, would not destroy the pore structure, and could supply a convenient way for separation of the adsorbent from water as well as the excellent resistibility to harsh environment. The physical and chemical properties of the synthesized material were studied, and the performance in heavy metal removal from natural water matrices was satisfying.

2. Experimental

2.1. Synthesis of SH-mSiO$_2$@Fe$_3$O$_4$

The Fe_3O_4 spherical particles were prepared according to the literature [23]. The thiol-functionalized SH-mSiO$_2$@Fe$_3$O$_4$ was prepared through a modified Stöber method [24]. Typically, 0.1 g of the prepared Fe_3O_4 spheres were treated with 0.1 M HCl aqueous solution under ultrasonication for at least 10 min. After separation and washing with deionized water, the magnetic spheres were dispersed in a mixed solution of 80 mL ethanol, 20 mL deionized water and 1 mL concentrated ammonia aqueous solution (28%) under vigorous stirring. Then 0.05 g tetraethyl orthosilicate (TEOS, Thermo Fisher Scientific) was added dropwise. After magnetically stirred at room temperature for 6 h, the product was separated and washed with ethanol and deionized water, and then redispersed in a solution containing 0.3 g cetyltrimethylammonium bromide (CTAB, Amresco), 70 mL deionized water, 70 mL absolute ethanol and 1.1 mL concentrated ammonia aqueous solution

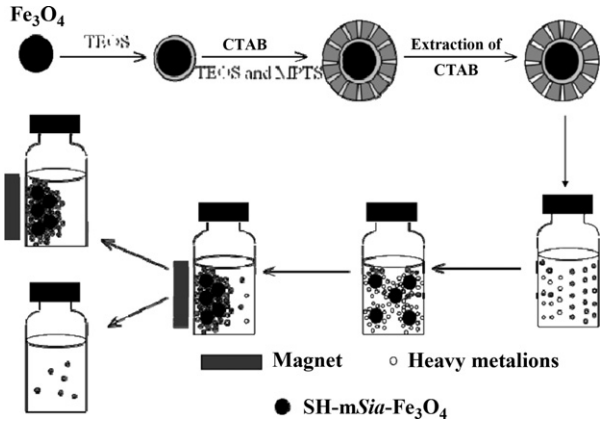

Fig. 1. Synthesis route of SH-mSi@Fe_3O_4 and its use for heavy metal ions removal.

(28%). The mixture was homogenized under ultrasonication for 30 min, followed by dropwise addition of the mixture of 3.2 g TEOS and 0.9 g (3-mercaptopropyl)-trimethoxysilane (MPTS, Alfa Aesar) under vigorous stirring. After 6 h stirring, the product was collected by magnetic separation and repeatedly washed with ethanol and deionized water to remove nonmagnetic byproducts. The structure-directing agent CTAB was thereafter removed with acetone reflux at 80 °C. The whole synthesis procedure is presented in Fig. 1. The product was vacuum-dried at 60 °C overnight and placed in a desiccator before use.

2.2. Characterization

The morphology of the SH-mSi@Fe_3O_4 was observed through a scanning electron microscopy (Hitachi S-3000N) equipped with an energy dispersive X-ray spectroscope (EDS) and a transmission electron microscopy (Hitachi H-800) performed at an accelerating voltage of 100 kV. A Fourier transform infrared (FT-IR) spectrometry performed on 80OOs with KBr disks of powdered samples was used to identify the functional groups of SH-mSiO$_2$@Fe_3O_4. Powder X-ray diffraction pattern of the material was recorded with a PANalytical X'Pert Pro X-ray diffractometer using Cu-Kα radiation over 2θ range from 1° to 10°. The N_2 adsorption–desorption isotherm was determined using a Micromeritics ASAP-2000 at 77 K after the adsorbent was dehydrated and degassed at 120 °C for 3 h. The surface area and the pore distribution were calculated by Brunauer–Emmett–Teller (BET) and Barret–Joyner–Halenda (BJH) equations. The magnetic property was measured using a magnetometer (NIM-200C, National Institute of Metrology, China) at room temperature.

2.3. Adsorption kinetics

A volume of 100 mL aqueous solutions containing Hg^{2+} and Pb^{2+} at concentration of 1 mg/L for each was transferred to capped polypropylene bottles. The solutions were adjusted to pH 6.5 ± 0.05 using 0.1 M HNO_3 and NaOH. After 1 mg of SH-mSi@Fe_3O_4 was added, the solutions were agitated on a rotatory oscillator at 200 rpm at room temperature (25 °C). Samples were pipetted at certain intervals and the adsorbent was separated using a magnet. The sample solutions were then spiked with HNO_3 to 3% (v/v) and injected to ICP-MS for analysis.

The pseudo-second-order kinetics was used to evaluate the sorption kinetics and calculate the rate constants, initial sorption rates and adsorption capacities:

$$\frac{t}{q_t} = \frac{1}{k_{ad}q_e^2} + \frac{1}{q_e}t \quad (1)$$

where k_{ad} (g/mmol min) is the rate constant of adsorption, q_e (mmol/g) is the equilibrium adsorption capacity, q_t (mmol/g) is the amounts of metal adsorbed at time t.

The intraparticle diffusion rate was defined as [25,26]:

$$q = k_{id}t^{0.5} \quad (2)$$

where q is the amount of heavy metals removed, k_{id} stands for the intraparticle diffusion constant.

2.4. Adsorption isotherm

A series of 100 mL solutions containing Hg^{2+} and Pb^{2+} with concentrations of 0, 1, 2, 4 and 6 mg/L (pH 6.5 ± 0.05) were added with 1 mg of SH-mSi@Fe_3O_4 and agitated in an rotator oscillator at 25 °C for 5 h to study the adsorption isotherm of the adsorbent. The solutions were sampled and analyzed as described above.

Langmuir and Freundlich equations were used to evaluate adsorption isotherm. The Langmuir equation is defined as:

$$q_e = \frac{bq_mC_e}{1 + bC_e} \quad (3)$$

where q_e is the adsorption capacity at equilibrium (mmol/g adsorbent), C_e is the equilibrium concentration of heavy metals (mg/L), q_m and b are the maximum adsorption capacity (mmol/g) and the equilibrium adsorption constant (L/mmol).

The Freundlich equation is defined as:

$$\log q_e = \log k + \frac{1}{n}\log C_e \quad (4)$$

where k and n are the Freundlich constants.

2.5. Distribution coefficient (K_d) measurement

The tested matrices included tap water (Beijing, China), ground water (Qingdao, China), sea water from Bohai bay (Qingdao, China), lake water (Wuhan, China) and river water from Yangtze River (Wuhan, China). All samples were filtered with 0.45 μm micron cellulose membranes and spiked with Hg^{2+}, Pb^{2+}, Ag^{+} and Cu^{2+} to final concentrations of 100 μg/L. Aliquots of 10 mL samples were filled into series of 15 mL of capped polypropylene bottles followed by addition of 0.1 mg SH-mSi@Fe_3O_4 and agitated in a rotatory oscillator at 200 rpm at room temperature (25 °C) for 5 h. The samples were then placed on a magnet to separate the adsorbent from the sample solution. The supernatant was pipetted for analysis. K_d was calculated with the equation as below [27]:

$$K_d = \left(\frac{C_0 - C_f}{C_f}\right) \times \left(\frac{V}{M}\right) \quad (5)$$

where C_0 and C_f represent the initial and final concentrations of ions in the solution. V and M represent the solution volume (mL) and the mass of the adsorbent (g), respectively.

3. Results and discussion

3.1. Characterization of the SH-mSi@Fe_3O_4

The N_2 adsorption–desorption isotherm can be categorized as type IV curve, with a distinct hysteresis loop observed in the range of 0.45–1.0 P/P_0 [28]. The average pore diameter was 2.5 nm. The BET area and total pore volume were calculated to be 321 m^2/g and 0.29 cm^3/g, respectively. The small angle X-ray diffraction pattern (SAXRD) of the SH-mSi@Fe_3O_4 (Fig. S1 of supplementary information) shows only one peak at 2θ degree of 2.55, indicating the wormhole-like pore structure within the prepared mesoporous framework, rather than long-range mesopore channels [29]. This is probably due to the cross-linked organic group being homogeneously distributed in the silica matrix, which results in less condensed organic-silica framework [30–32]. Fourier infrared spectrum (Fig. 2) shows the characteristic peaks of the SH-mSi@Fe_3O_4 at 890 cm^{-1} (Si–C), 1090 cm^{-1} (Si–O stretch of Si–O–Me), 2825 cm^{-1} (C–H stretches of O–CH_3), and 2935 cm^{-1} (normal C–H stretch of propyl). The double peaks of S–H were found at 2358 and 2345 cm^{-1}, which are typically very weak due to the aggregation of mercapto groups within the monolayer and hydrogen binding effects. The absorption bands at 586 and 636 cm^{-1} are usually attributed to the Fe–O stretches [27,33].

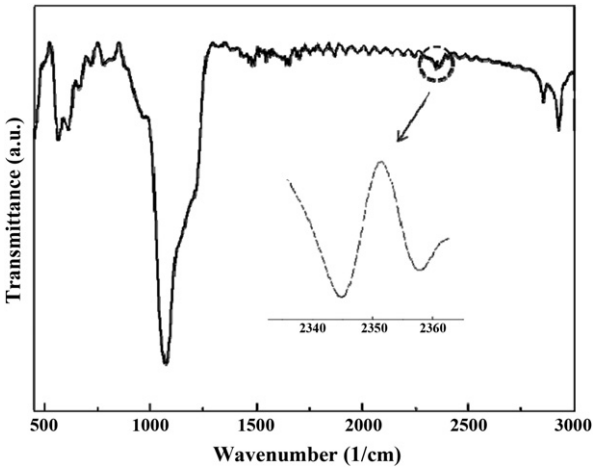

Fig. 2. Fourier transform-infrared (FT-IR) spectrum of SH-mSi@Fe_3O_4.

Both SEM and TEM images (Fig. 3) illustrate the spherical morphology of SH-mSi@Fe_3O_4. The average diameter of the particles is around 500 nm. It is observed from Fig. 3b that the skirt of the particles is lighter than the central part, indicating the less compact outer mesoporous shell and the condensed inner magnetic cores. Element mass contents of Si, S and Fe (Fig. S2 of supplementary information) in SH-mSi@Fe_3O_4 were 17.95%, 1.23% and 38.03%, respectively.

3.2. Adsorption kinetics and intraparticle diffusion rate

Hg^{2+} and Pb^{2+} were used as target analytes to investigate the adsorption kinetics of heavy metals on SH-mSi@Fe_3O_4. Fig. 4a shows that adsorption of Hg^{2+} and Pb^{2+} is a time-dependent process. The adsorption process was very rapid in the first 20 min, and then decreased considerably until equilibrium was achieved. More time was needed for Pb^{2+} to reach the same residual concentration as Hg^{2+}, which meant that adsorption of Hg^{2+} by SH-mSi@Fe_3O_4 was much easier than Pb^{2+}. The adsorption of Hg^{2+} and Pb^{2+} fitted well with pseudo-second-order kinetic equation (insetted picture in Fig. 4a), the constant k_{ad} was calculated and listed in Table 1.

To further evaluate the adsorption process, the rate constant for intraparticle diffusion (k_{id}) was introduced [34,35]. Fig. 4b shows the plots of q versus $t^{0.5}$ for Hg^{2+} and Pb^{2+}. It is observed from the plot there are three regions depicting the mass transfer on the SH-mSi@Fe_3O_4. The intraparticle diffusion constants could be

Table 1
Pseudo-second order rate constants and intraparticle diffusion rates.

	Pseudo-second order rate	Intraparticle diffusion rate		
	k_{ad} (g/mmol min)	$k_{id.1}$	$k_{id.2}$	$k_{id.3}$ (g/mmol $h^{0.5}$)
Hg	0.623	0.887	0.357	0.005
Pb	0.430	0.712	0.161	0.043

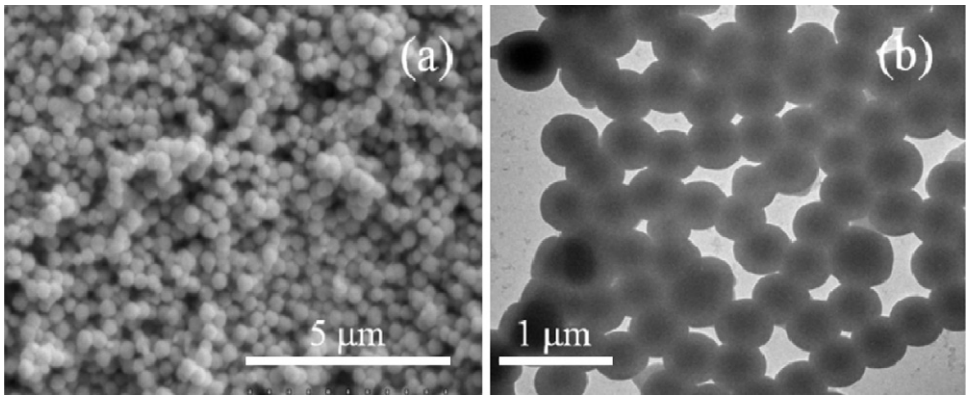

Fig. 3. Images of scanning electron microscopy (SEM) and the transmission electron microscopy (TEM) of SH-mSi@Fe_3O_4.

determined from the slop of the plots. The $k_{id.1}$, $k_{id.2}$, and $k_{id.3}$ which express the diffusion rates of the different stages in adsorption process are tabulated in Table 1. The adsorption rate is in the order of $k_{id.1} > k_{id.2} > k_{id.3}$. Both metals underwent firstly a steep-sloped stage, followed by the decreasing slope and the subsequent plateau till equilibrium. The first steep-sloped period is the instantaneous diffusion stage ($k_{id.1}$, from 0 to 0.15 h), during which a large amount of heavy metal ions (about 50%) were rapidly adsorbed by the exterior surface of the adsorbent. When the adsorption of exterior surface reached saturation, metal ions entered into the pores of the adsorbent and were adsorbed by the interior surface of the mesopores. With the heavy metal ions entering into the pores, the diffusion resistance increased, leading to decrease of the diffusion rate ($k_{id.2}$). With the rapid decrease of the solute concentration, the intraparticle diffusion rate gradually slowed down and finally reached the equilibrium stage ($k_{id.3}$) [26].

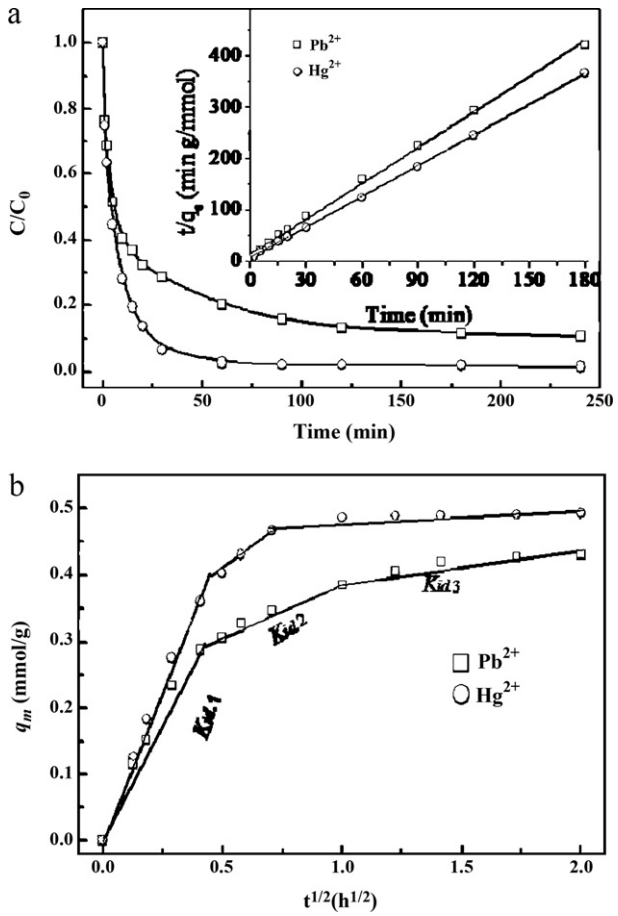

Fig. 4. (a) Adsorption kinetics of SH-mSi@Fe_3O_4 in aqueous solution of Hg^{2+} and Pb^{2+}, the insetted picture is the pseudo-second-order adsorption rates. (b) The intraparticle rate of adsorption of Hg^{2+} and Pb^{2+} to SH-mSi@Fe_3O_4 (concentrations of metal ions (1 mg/L), adsorbent loading (1 mg/100 mL), pH (6.5 ± 0.05), and temperature (25 °C)).

3.3. Adsorption isotherm

Adsorption isotherm is important for determining the adsorption behavior of an adsorbent. Therefore, Hg^{2+} and Pb^{2+} were selected as models to determine the adsorption isotherm type of SH-mSi@Fe_3O_4. Fig. 5 shows the adsorption isotherm at pH 6.5 ± 0.05 for the adsorbent. The isotherm curves demonstrate the adsorption as a function of the equilibrium concentration of metal ions in solution. Both Langmuir and Freundlich adsorption isotherms were used to normalize the adsorption data. The results are summarized in Table 2. The results showed that Langmuir model fitted better than the Freundlich model, demonstrating that the adsorption of Hg^{2+} and Pb^{2+} onto SH-mSi@Fe_3O_4 can be considered to be a monolayer adsorption process. The adsorption capacity of Hg^{2+} and Pb^{2+} were calculated to be 1.3 and 0.44 mmol/g, respectively. Taking adsorption of Hg^{2+} for example, the adsorption capacity of SH-mSi@Fe_3O_4 is not only higher than some thiol functionalized ordered mesoporous silica prepared through the co-condensing method (0.16 and 0.12 mmol/g of Hg^{2+} for MP-SBA-15 and MP-MCM-41) [36], but also higher than the reported thiol func-

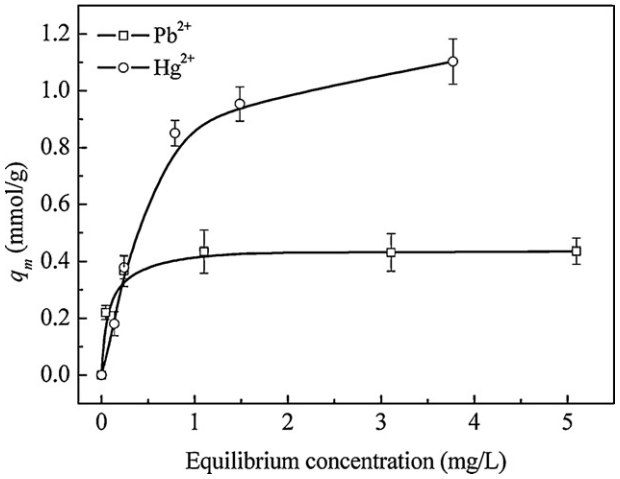

Fig. 5. Hg^{2+} and Pb^{2+} adsorption isotherms of SH-mSi@Fe_3O_4 (initial concentrations from 0 to 6 mg/L, adsorbent loading (1 mg/100 mL), pH (6.5 ± 0.05), and temperature (25 °C)).

Table 2
Parameters of adsorption isotherms of Hg and Pb on SH-mSi@Fe_3O_4.

Adsorption isotherms and parameters	Hg	Pb
Langmuir		
b (L/mmol)	1.83	22.3
q_m (mmol/g)	1.31	0.442
R^2	0.985	0.999
Freundlich		
K (mmol$^{1-1/n}$ L$^{1/n}$/g)	0.736	0.389
n	2.69	8.14
R^2	0.917	0.964

tionalized nanoporous silica (not more than 0.6 mmol/g) [21] and some other adsorbents [37,38].

3.4. Effect of pH

The uptake capacity of an adsorbent for metal ions not only depends on the chemical and physical properties of the adsorbent and the target metal ions, but also on the conditions of sample matrix such as the hydrolysis capacity of the metal ions and the competitive adsorption of coexisting matters in aqueous samples [27,39,40]. The pK_a of the ligand and the stability of the ligand–metal complex correlate with the pH value of the solution. Alkaline conditions hinder the removal of some heavy metals due to formation of stable hydroxyl complexes or hydroxides [40]. In order to investigate the effect of pH on the adsorption of heavy metal ions, SH-mSi@Fe_3O_4 was mixed with solutions containing 200 μg/L of Hg, Ag, Pb, and Cu ions at different pH values. The concentrations of metal ions in the solutions were detected after 5 h adsorption and the results are shown in Fig. 6.

It was observed that the removal efficiencies of the tested metal ions on SH-mSi@Fe_3O_4 have a tendency of $Ag^+ \approx Hg^{2+} > Pb^{2+} > Cu^{2+}$ in the pH range of 5–7, which could be explained by Pearson's theory that soft ligands like the thiol group are more likely to bind with soft metals, and Hg and Ag are considered to be softer than Pb and Cu [41]. It was also observed that an increasing amount of metal ions could be adsorbed at relatively higher pH. Metal cations have tendency to hydrate in aqueous solution with the increase of the pH value. It was reported that the effective sizes of hydrated species of metal ions in aqueous solution are in the order of $M^{2+} > M(OH)^+ > M(OH)_2$, depending on the charges of the species [42]. The mobility of the hydrated species with smaller effective size is higher in comparison with larger hydrated M^{2+} species, thus resulting in increased adsorption during adsorbate/adsorbent interaction with the increase of the pH value. The decrease of adsorption with decreasing solution pH is thereby attributed to (i) low mobility of bigger hydrated species (M^{2+}) and (ii) competition of H^+ for available surface sites and the strengthening protonation of the –SH group (pK_a 9.65) in stronger acid condition.

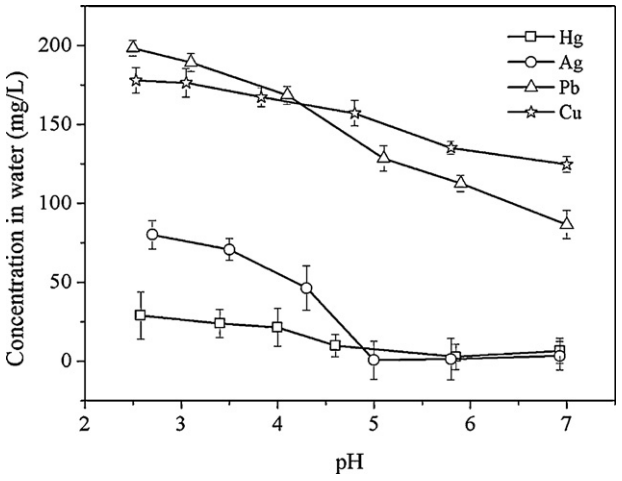

Fig. 6. Effect of pH on the removal of heavy metals by the SH-mSi@Fe_3O_4 (initial concentration of metal ions (200 μg/L), adsorbent loading (1 mg/100 mL), and temperature (25 °C), pH was adjusted by 0.1 M HNO_3 and NaOH).

3.5. Effect of natural water matrices

Natural waters are very complicated matrices, containing various inorganic and organic substances. These constituents are able to interact with the adsorbents used in water purification. To study the availability and the effectiveness of SH-mSi@Fe_3O_4 on the uptake of heavy metal ions in natural water sources, different water matrices spiked with single metal ion were mixed with the adsorbent. The removal efficiencies for single metal ion were determined after the adsorption.

It was found from Table 3 that SH-mSi@Fe_3O_4 exerted good adsorption for Hg^{2+}, Pb^{2+} and Ag^+ in different natural water sources, with removal efficiencies of over 95%. While, adsorption of Cu^{2+} was the worst with the removal efficiency not more than 80%. The distribution coefficient (K_d) between water and the adsorbent is also used to evaluate the adsorption performance in different water matrices [27]. The K_d values of the metal ions in tested water matrices were at the magnitude of 10^5, which is much higher than the value of 10^3 categorized as good performance [43].

It is also found that the SH-mSi@Fe_3O_4 adsorbed more heavy metals from groundwater than from other water sources. This is probably due to the groundwater used in the experiment contains less competing metal cations like Ca^{2+} and Mg^{2+} and organic matter (total organic carbon, TOC). Although the affinity to thiol group is weak, Ca^{2+} and Mg^{2+} could still bind with a portion of the adsorption sites on the surface of SH-mSi@Fe_3O_4 through Coulomb force. Organic matters also have strong effect on heavy metal removal. Suspended large molecular organic substances could block the pores of the mesoporous adsorbents, which leads to the decrease of adsorption efficiency on the one hand, and organic functional groups like carboxylate and hydroxylate could counteract the adsorption on the other [44]. Therefore, the performance of SH-mSi@Fe_3O_4 in groundwater was better.

3.6. Effect of coexisting metal ions

The competitive adsorption of coexisting ions to the binding sites is usually a severe problem when using conventional adsorbents for removal of heavy metals. To investigate the effect of coexisting ions, the uptake capacities of SH-mSi@Fe_3O_4 in different water matrices with mixed heavy metal ions were tested.

Fig. 7 shows the competitive adsorption between Hg^{2+}, Pb^{2+}, Ag^+ and Cu^{2+} in different water matrices. The residue concentration of Cu^{2+} was higher than that of other three metal ions because of its weak affinity to thiol group. However, the removal efficiency of Cu^{2+} was still more than 70% which was higher than that in natural water matrices with single metal ion in the same experimental condition. This suggested that coexisting heavy metals facilitated the adsorption of Cu^{2+} to SH-mSi@Fe_3O_4. This phenomenon can be explained as below: the organic moieties embedded in the pore walls endue the adsorbent surface with hydrophobic characteristic. While upon vigorous shaking, contact between the adsorbent and the bulk solution occurred. The heavy metal ions with strong affinity to –SH such as Hg^{2+} and Ag^+ first bind with –SH groups near the orifice of the pores and created a hydrophilic threshold leading to more aqueous solution entering into the pores [45]. Therefore, more –SH binding sites become accessible even to those ions with weaker affinity. The other reason may be the inherent random networks with broad pore size distribution of the organic–inorganic

Table 3
The removal efficiencies of tested heavy metal ions by SH-mSi@Fe_3O_4 from different water samples and the calculated distribution coefficients (K_d, mL/g) of ions between water matrices and the SH-mSi@Fe_3O_4. The initial concentrations of Hg^{2+}, Pb^{2+}, Ag^+ and Cu^{2+} were 100 μg/L, respectively. The pH values, TOC, concentrations of Mg^{2+} and Ca^{2+} in the water were also detected to evaluate the selected matrices.

Matrices	pH	TOC (mg/L)	Mg^{2+} (mg/L)	Ca^{2+} (mg/L)	Hg^{2+}		Pb^{2+}		Ag^+		Cu^{2+}	
					Removal efficiency (%)	$K_d \times 10^{-5}$	Removal efficiency (%)	$K_d \times 10^{-5}$	Removal efficiency (%)	$K_d \times 10^{-5}$	Removal efficiency (%)	$K_d \times 10^{-5}$
River water	7.82	3.58	31.8	97.8	97.5	39.7	97.4	37.5	95.3	20.4	66.0	1.94
Lake water	7.77	6.87	10.4	40.4	98.3	58.7	97.7	43.2	99.1	66.6	66.7	2.0
Ground water	7.62	1.12	3.48	16.4	99.0	107	98.1	51.1	98.5	71.2	76.9	3.33
Tap water	7.78	3.18	18.2	49.0	97.6	40.4	97.4	37.8	95.2	20	54.8	1.21

hybrid mesoporous materials, which lead to an increase in entropy and thus benefit the diffusion of the metal ions [21].

3.7. Stability and reclamation

Stability in different conditions is important for the feasible application of an adsorbent. Furthermore, leaching of adsorbent components to water environment may induce secondary contamination. The iron of bare Fe_3O_4 core is easier to leach into the aqueous solution than those containing a shield coating [44]. For SH-mSi@Fe_3O_4, a thin layer of coated silica helped Fe_3O_4 to resist harsh conditions. No iron ion leached after the adsorbent was dispersed in natural water samples for 48 h. The percentage of leached iron in 0.1 M HCl and NaOH aqueous solutions were 0.422 and 0.425%, respectively. There were just 12.47 and 8.88% of iron leached in extreme strong acid (1 M HCl) and alkaline (1 M NaOH) conditions after 48 h (Table S1 in supplementary information). Therefore, it can be expected that this material is stable in natural water matrices and wastewater even under extreme conditions.

Fig. 8 shows that the saturation magnetizations of SH-mSi@Fe_3O_4 and Fe_3O_4 were 38.4 and 75.5 emu/g, respectively. The absence of remanence confirm the superparamagnetism of SH-mSi@Fe_3O_4, and the magnetization property enables the adsorbent to be easily separated from aqueous solution under a magnetic field in less than 30 s. As SH-mSi@Fe_3O_4 is resistant to relatively strong acid solutions, SH-mSi@Fe_3O_4 loaded with Hg^{2+} which shows strong affinity to thiol group was treated in 1 M HCl under sonication for 30 min. Results showed that 91% of the adsorbed Hg could

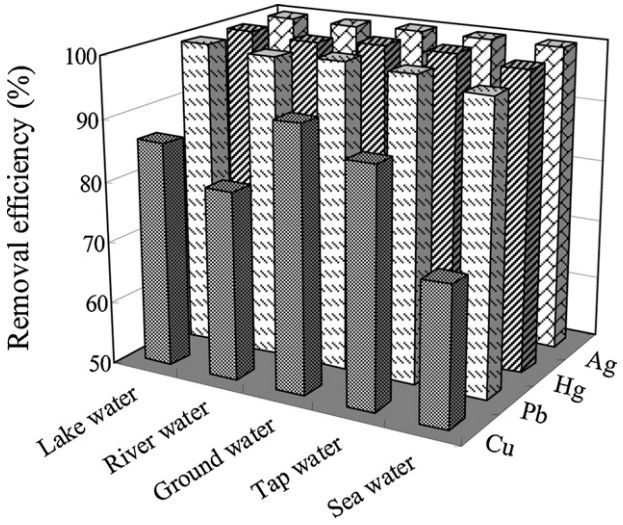

Fig. 7. The removal efficiency of heavy metals in different water matrices (the water matrices contained mixed Hg^{2+}, Pb^{2+}, Ag^+, and Cu^{2+} with initial concentration of 200 μg/L for each metal ion, adsorbent loading (1 mg/100 mL), temperature (25 °C)).

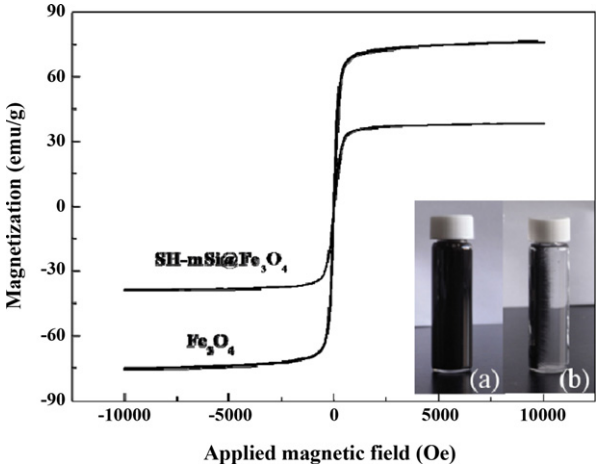

Fig. 8. The magnetization curves of Fe_3O_4 and SH-mSi@Fe_3O_4, and the photos of SH-mSi@Fe_3O_4 before (a) and after (b) separation from solution in magnetic field.

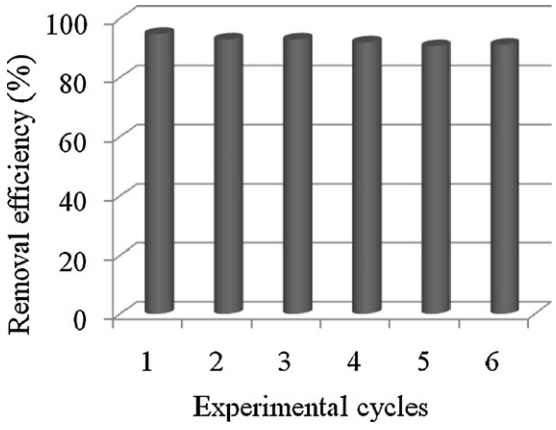

Fig. 9. Removal efficiency of Hg^{2+} in different cycles by SH-mSi@Fe_3O_4 (concentration of Hg^{2+} in every cycle was 1 mg/L, adsorbent loading (1 mg/100 mL), pH (6.5 ± 0.05), and temperature (25 °C)).

be released. Then, the regenerated adsorbent was treated with deionized water to neutralize for adsorption of Hg^{2+} in succeeding cycles. We have repeated the above procedure for six cycles. As shown in Fig. 9, the removal efficiency is slightly reduced in the subsequent cycles. However, it is still above 90% in the sixth cycle.

4. Conclusion

A new adsorbent for heavy metal removal was successfully prepared in this paper. Such prepared adsorbent has not only the wormhole like mesopore structure with large surface area and pore volume, but also the superparamagnetic character. These features

make it an effective and convenient adsorbent for heavy metal removal. The adsorption kinetics abides by pseudo second order kinetic equation. The adsorption process could be well described by intraparticle diffusion model and the adsorption rate of heavy metals on this adsorbent was mainly controlled by the diffusion rate within the pore. The adsorption process fitted well with Langmuir isotherm. The prepared adsorbent performed better in neutral pH condition, and was stable in strong acid and alkaline condition. This adsorbent could be used in different water sources such as river water, lake water, groundwater and tap water. The presence of coexisting heavy metal ions avail heavy metal adsorption. In conclusion, this thiol functionalized magnetic mesoporous silica is a promising adsorbent for heavy metal removal from water.

Acknowledgments

This work was jointly supported by the National Basic Research Program of China (No. 2009CB421605, 2011CB936001), the National Natural Science Foundation of China (No. 20890111) and National Key Water Program (2009ZX07527-005).

Appendix A. Supplementary data

Supplementary data associated with this article can be found, in the online version, at doi:10.1016/j.jhazmat.2011.05.015.

References

[1] L. Jarup, Hazards of heavy metal contamination, Br. Med. Bull. 68 (2003) 167–182.
[2] W. Plazinski, W. Rudzinski, Modeling the effect of surface heterogeneity in equilibrium of heavy metal ion biosorption by using the ion exchange model, Environ. Sci. Technol. 43 (2009) 7465–7471.
[3] M.Y. Vilensky, B. Berkowitz, A. Warshawsky, In situ remediation of groundwater contaminated by heavy- and transition-metal ions by selective ion-exchange methods, Environ. Sci. Technol. 36 (2002) 1851–1855.
[4] S. Coruh, G. Senel, O.N. Ergun, A comparison of the properties of natural clinoptilolites and their ion-exchange capacities for silver removal, J. Hazard. Mater. 180 (2010) 486–492.
[5] M.A. Hasan, Y.T. Selim, K.M. Mohamed, Removal of chromium from aqueous waste solution using liquid emulsion membrane, J. Hazard. Mater. 168 (2009) 1537–1541.
[6] B. Yu, Y. Zhang, A. Shukla, S.S. Shukla, K.L. Dorris, The removal of heavy metal from aqueous solutions by sawdust adsorption—removal of copper, J. Hazard. Mater. 80 (2000) 33–42.
[7] M.K. Doula, Removal of Mn^{2+} ions from drinking water by using Clinoptilolite and a Clinoptilolite–Fe oxide system, Water Res. 40 (2006) 3167–3176.
[8] M.K. Doula, Simultaneous removal of Cu, Mn and Zn from drinking water with the use of clinoptilolite and its Fe-modified form, Water Res. 43 (2009) 3659–3672.
[9] W. Mozgawa, M. Krol, W. Pichor, Use of clinoptilolite for the immobilization of heavy metal ions and preparation of autoclaved building composites, J. Hazard. Mater. 168 (2009) 1482–1489.
[10] M.C. Burleigh, M.A. Markowitz, M.S. Spector, B.P. Gaber, Amine-functionalized periodic mesoporous organosilicas, Chem. Mater. 13 (2001) 4760–4766.
[11] Y. Miyake, M. Yosuke, E. Azechi, S. Araki, S. Tanaka, Preparation and adsorption properties of thiol-functionalized mesoporous silica microspheres, Ind. Eng. Chem. Res. 48 (2009) 938–943.
[12] D.A. Loy, J.V. Beach, B.M. Baugher, R.A. Assink, K.J. Shea, J. Tran, J.H. Small, Dialkylene carbonate-bridged polysilsesquioxanes. Hybrid organic–inorganic sol-gels with a thermally labile bridging group, Chem. Mater. 11 (1999) 3333–3341.
[13] H. Sepehrian, S. Waqif-Husain, M. Ghannadi-Maragheh, Development of thiol-functionalized mesoporous silicate MCM-41 as a modified sorbent and its use in chromatographic separation of metal ions from aqueous nuclear waste, Chromatographia 70 (2009) 277–280.
[14] A.M. Liu, K. Hidajat, S. Kawi, D.Y. Zhao, A new class of hybrid mesoporous materials with functionalized organic monolayers for selective adsorption of heavy metal ions, Chem. Commun. (2000) 1145–1146.
[15] M.C. Burleigh, S. Dai, E.W. Hagaman, J.S. Lin, Imprinted polysilsesquioxanes for the enhanced recognition of metal ions, Chem. Mater. 13 (2001) 2537–2546.
[16] F. Hoffmann, M. Cornelius, J. Morell, M. Froba, Silica-based mesoporous organic–inorganic hybrid materials, Angew. Chem., Int. Ed. 45 (2006) 3216–3251.
[17] E.F.S. Vieira, J.D. Simoni, C. Airoldi, Interaction of cations with SH-modified silica gel: thermochemical study through calorimetric titration and direct extent of reaction determination, J. Mater. Chem. 7 (1997) 2249–2252.
[18] M.H. Lim, A. Stein, Comparative studies of grafting and direct syntheses of inorganic–organic hybrid mesoporous materials, Chem. Mater. 11 (1999) 3285–3295.
[19] M.H. Lim, C.F. Blanford, A. Stein, Synthesis of ordered microporous silicates with organosulfur surface groups and their applications as solid acid catalysts, Chem. Mater. 10 (1998) 467–470.
[20] J. Brown, R. Richer, L. Mercier, One-step synthesis of high capacity mesoporous Hg^{2+} adsorbents by non-ionic surfactant assembly, Microporous Mesoporous Mater. 37 (2000) 41–48.
[21] J. Brown, L. Mercier, T.J. Pinnavaia, Selective adsorption of Hg^{2+} by thiol-functionalized nanoporous silica, Chem. Commun. 1 (1999) 69–70.
[22] J.A. Liu, S.Z. Qiao, Q.H. Hu, G.Q. Lu, Magnetic nanocomposites with mesoporous structures: synthesis and applications, Small 7 (2011) 425–443.
[23] H. Deng, X.L. Li, Q. Peng, X. Wang, J.P. Chen, Y.D. Li, Monodisperse magnetic single-crystal ferrite microspheres, Angew. Chem., Int. Ed. 44 (2005) 2782–2785.
[24] W. Stöber, A. Fink, E. Bohn, Controlled growth of monodisperse silica spheres in micron size range, J. Colloid Interface Sci. 26 (1968) 62–69.
[25] C. Namasivayam, K. Ranganathan, Removal of Cd(II) from waste-water by adsorption on waste Fe(III)/Cr(III) hydroxide, Water Res. 29 (1995) 1737–1744.
[26] Q.Y. Sun, L.Z. Yang, The adsorption of basic dyes from aqueous solution on modified peat-resin particle, Water Res. 37 (2003) 1535–1544.
[27] W. Yantasee, C.L. Warner, T. Sangvanich, R.S. Addleman, T.G. Carter, R.J. Wiacek, G.E. Fryxell, C. Timchalk, M.G. Warner, Removal of heavy metals from aqueous systems with thiol functionalized superparamagnetic nanoparticles, Environ. Sci. Technol. 41 (2007) 5114–5119.
[28] K.S.W. Sing, D.H. Everett, R.A.W. Haul, L. Moscou, R.A. Pierotti, J. Rouquerol, T. Siemieniewska, Reporting physisorption data for gas solid systems with special reference to the determination of surface-area and porosity (recommendations 1984), Pure Appl. Chem. 57 (1985) 603–619.
[29] S.J. Ding, B. Liu, C.L. Zhang, Y. Wu, H.F. Xu, X.Z. Qu, J.G. Liu, Z.Z. Yang, Amphiphilic mesoporous silica composite nanosheets, J. Mater. Chem. 19 (2009) 3443–3448.
[30] T. Asefa, M.J. MacLachlan, N. Coombs, G.A. Ozin, Periodic mesoporous organosilicas with organic groups inside the channel walls, Nature 402 (1999) 867–871.
[31] S. Guan, S. Inagaki, T. Ohsuna, O. Terasaki, Cubic hybrid organic–inorganic mesoporous crystal with a decaoctahedral shape, J. Am. Chem. Soc. 122 (2000) 5660–5661.
[32] D. Chen, L.L. Li, F.Q. Tang, S.O. Qi, Facile and scalable synthesis of tailored silica "nanorattle" structures, Adv. Mater. 21 (2009) 3804–3807.
[33] Y.W. Jun, Y.M. Huh, J.S. Choi, J.H. Lee, H.T. Song, S. Kim, S. Yoon, K.S. Kim, J.S. Shin, J.S. Suh, J. Cheon, Nanoscale size effect of magnetic nanocrystals and their utilization for cancer diagnosis via magnetic resonance imaging, J. Am. Chem. Soc. 127 (2005) 5732–5733.
[34] B. Manna, U.C. Ghosh, Adsorption of arsenic from aqueous solution on synthetic hydrous stannic oxide, J. Hazard. Mater. 144 (2007) 522–531.
[35] S.J. Allen, G. McKay, K.Y.H. Khader, Intraparticle diffusion of a basic dye during adsorption onto sphagnum peat, Environ. Pollut. 56 (1989) 39–50.
[36] D. Perez-Quintanilla, I. del Hierro, M. Fajardo, I. Sierra, Mesoporous silica functionalized with 2-mercaptopyridine: synthesis, characterization and employment for Hg(II) adsorption, Microporous Mesoporous Mater. 89 (2006) 58–68.
[37] K. Ranganathan, Adsorption of Hg(II) ions from aqueous chloride solutions using powdered activated carbons, Carbon 41 (2003) 1087–1092.
[38] M. Monier, D.M. Ayad, A.A. Sarhan, Adsorption of Cu(II), Hg(II), and Ni(II) ions by modified natural wool chelating fibers, J. Hazard. Mater. 176 (2010) 348–355.
[39] X.W. Liu, Q.Y. Hu, Z. Fang, X.J. Zhang, B.B. Zhang, Magnetic chitosan nanocomposites: a useful recyclable tool for heavy metal ion removal, Langmuir 25 (2009) 3–8.
[40] M.Q. Yu, W. Tian, D.W. Sun, W.B. Shen, G.P. Wang, N. Xu, Systematic studies on adsorption of 11 trace heavy metals on thiol cotton fiber, Anal. Chim. Acta 428 (2001) 209–218.
[41] R.G. Pearson, Hard and soft acids and bases, J. Am. Chem. Soc. 85 (1963) 3533–3539.
[42] B. Xiao, K.M. Thomas, Adsorption of aqueous metal ions on oxygen and nitrogen functionalized nanoporous activated carbons, Langmuir 21 (2005) 3892–3902.
[43] G.E. Fryxell, Y.H. Lin, S. Fiskum, J.C. Birnbaum, H. Wu, K. Kemner, S. Kelly, Actinide sequestration using self-assembled monolayers on mesoporous supports, Environ. Sci. Technol. 39 (2005) 1324–1331.
[44] J.F. Liu, Z.S. Zhao, G.B. Jiang, Coating Fe_3O_4 magnetic nanoparticles with humic acid for high efficient removal of heavy metals in water, Environ. Sci. Technol. 42 (2008) 6949–6954.
[45] I.L. Lagadic, M.K. Mitchell, B.D. Payne, Highly effective adsorption of heavy metal tons by a thiol-functionalized magnesium phyllosilicate clay, Environ. Sci. Technol. 35 (2001) 984–990.